Lewis Acid Induced [2+2] Cycloadditions of Silyl Enol Ethers with α,β-Unsaturated Esters: A DFT Analysis

Manuel Arnó,[a] Ramón J. Zaragozá,[a] and Luis R. Domingo*[a]

Keywords: Cycloaddition / Density functional calculations / Electrophilicity / Lewis acids

The Lewis acid (LA) induced cycloaddition of trimethysilyl vinyl ether with methyl acrylate has been studied by DFT methods at the B3LYP/6-31G* level. In the absence of an LA, a [4+2] cycloaddition between the silyl enol ether and methyl acrylate in the *s-cis* conformation takes place through an asynchronous, concerted bond-formation process. This cycloaddition presents a large activation enthalpy of 21.1 kcal mol^{-1}. Coordination of the LA $AlCl_3$ to the carbonyl oxygen atom of methyl acrylate yields a change of molecular mechanism from a concerted to a two-step mechanism and produces a drastic reduction of the activation energy. This stepwise mechanism is initialized by the nucleophilic attack of the enol ether at the β-position of methyl acrylate in a Michael-type addition. The very low activation energy (7.1 kcal mol^{-1}) associated with this nucleophilic attack can be related to the increase of the electrophilicity of the LA-coordinated α,β-unsaturated ester, which favors the cycloaddition through a polar process. The subsequent ring-closure allows the formation of the corresponding [2+2] and [4+2] cycloadducts. While the [4+2] cycloadduct is formed by kinetic control, the [2+2] cycloadducts are formed by thermodynamic control. The energetic results provide an explanation for the conversion of [4+2] cycloadducts into the thermodynamically more stable [2+2] ones. The *cis/trans* ratio found for the catalytic [2+2] process is in agreement with the experimental outcome.

Introduction

Cycloaddition reactions are one of the most important processes of both synthetic and mechanistic interest in organic chemistry.[1] In this type of reaction, two new σ bonds are formed at the ends of two interacting π systems along with the formation of a carbocycle system. These reactions have been mechanistically classified as pericyclic reactions,[2] and the feasibility of the processes has been related to the Woodward–Hoffmann rules.[3] According to these rules, thermal [2+2] cycloadditions are forbidden when they proceed through a supra-supra concerted reaction path. Although a concerted supra-antara process is allowed according to the symmetry rules, in general it is expected to have high activation energy because of large steric effects.

The [4+2] cycloaddition between 1,3-butadiene and ethylene is an allowed supra-supra concerted process,[2] but it only takes place under drastic conditions: after 17 h at 165 °C and 900 atm, it gives a yield of 78 %.[3a,4] Appropriate substitution on the diene or dienophile favors the cycloaddition. Different studies have shown that the substitution changes the mechanism from a nonpolar, synchronous, concerted one to a polar, highly asynchronous bond-formation process. In some cases, the substitution is able to stabilize the corresponding zwitterionic intermediate, and the cycloaddition takes place by a stepwise process.[5] This polar mechanism, which has also been found in [4+3],[6] [3+2],[7] and [2+2][8] cycloadditions appears to be alternative to the more accepted pericyclic model.

The thermal [2+2] cycloaddition of ketenes and related compounds has been studied theoretically.[9] However, thermal ethylene/ethylene[10] or acetylene/ethylene[11] [2+2] cycloadditions have received less attention theoretically. Recently, a DFT study of the regioselective [2+2] cycloaddition of the benzyne **1** with the ketene acetal **2** has been reported (see Scheme 1).[8] This formal [2+2] cycloaddition is a polar, stepwise process characterized by the nucleophilic attack of the ketene acetal **2** at the C1 position of the substituted benzyne **1**. The electrophilicity index, ω,[12] defined within DFT, has been used to classify a series of reagents currently present in Diels–Alder[13] and related cycloaddition reactions.[6,8,14] A good correlation between the difference in electrophilicity of the reagents, $\Delta\omega$, and the polar character of the process was found. The electrophilicity of benzyne is 1.95 eV. This value, which is larger than that evaluated for acetylene, ω = 0.54 eV, provides an explanation of the reactivity of the benzyne derivatives toward nucleophilic additions.[15] Note, however, that these polar cycloadditions demand the participation of a good nucleophile, such as enol ethers or ketene acetals.[8]

---

[a] Instituto de Ciencia Molecular (UIQOT), Departamento de Química Orgánica, Universidad de Valencia,
Dr Moliner 50, 46100 Burjassot, Valencia, Spain
E-mail: Domingo@utopia.uv.es

DOI: 10.1002/ejoc.200500188

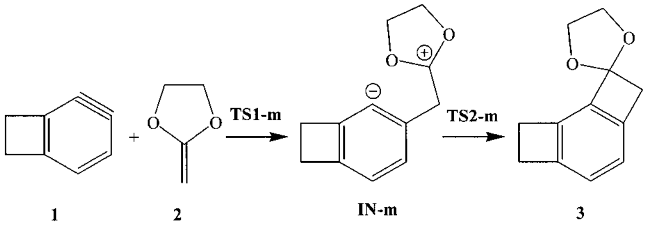

Scheme 1.

Takasu et al.[16] have reported recently that the catalytic [2+2] cycloaddition reactions of silyl enol ether **4** with the α,β-unsaturated esters **5** lead to the formation of a cyclobutane ring with a high degree of *trans* stereoselectivity (see Scheme 2). The results of stereochemical studies showed that the cycloaddition proceeds in a nonstereospecific manner, thus suggesting that the nucleophilic addition affords a short-lived zwitterionic intermediate.[16]

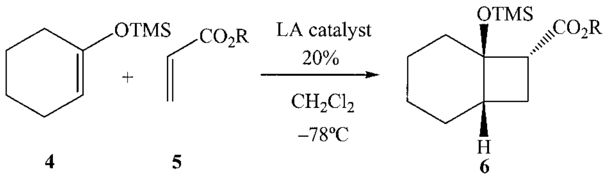

Scheme 2.

The role of Lewis acids (LAs) in cycloaddition reactions has been widely studied. Coordination of the LA to the electron-deficient reagent increases its electrophilicity notably, thus favoring the cycloaddition through a more polar process.[13] In the present work, the LA ($AlCl_3$) induced [2+2] cycloaddition between trimethylsilyl vinyl ether (SVE, **7**) and methyl acrylate (MA, **8**) is studied by DFT methods (see Scheme 3). Our purpose is to present these [2+2] cycloadditions as one case of the more general mechanism of the polar cycloadditions characterized by a nucleophile/electrophile interaction. It is noteworthy that these *pseudo-pericyclic reactions cannot be orbital symmetry forbidden*.[17] The study is performed by applying an analysis based on reactivity indexes defined in the context of DFT, and by exploring the potential energy surface (PES).

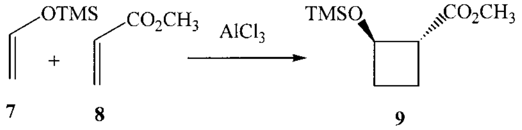

Scheme 3.

The Electrophilicity Index

The global electrophilicity index, ω, which measures the stabilization in energy when the system acquires an additional electronic charge, ΔN, from the environment, is given by the simple expression of Equation (1)[12] in terms of the electronic chemical potential, μ, and the chemical hardness η.

$$\omega = \frac{\mu^2}{2\eta} \qquad (1)$$

Both quantities may be expressed in terms of the one-electron energies of the frontier molecular orbital HOMO and LUMO, ε_H and ε_L, as $\mu \approx (\varepsilon_H + \varepsilon_L)/2$ and $\eta \approx \varepsilon_L - \varepsilon_H$, respectively.[18] The electrophilicity index encompasses both the propensity of the electrophile to acquire an additional electronic charge (driven by μ^2, the square of electronegativity) and the resistance of the system to exchange electronic charge with the environment described by η. A good electrophile is in this sense characterized by a high value of μ and a low value of η.

Beside the global electrophilicity index, it is possible to define its local (or regional) counterpart condensed to atoms.[19] The local electrophilicity index, ω_k, condensed to atom *k* is easily obtained by projecting the global quantity onto any atomic center *k* in the molecule by using the electrophilic Fukui function (i.e. the Fukui function for nucleophilic attack, f_k^+). This gives Equation (2).[19]

$$\omega_k = f_k^+ \omega \qquad (2)$$

Results and Discussions

DFT Analysis Based on Reactivity Indices

The electronic chemical potential, μ, the chemical hardness, η, and the global electrophilicity, ω, for SVE (**7**), MA (**8**), and the MA–LA complex **13** are presented in Table 1. The electronic chemical potential, μ, of SVE, μ = –0.0881 au, is less than the electronic chemical potential of the α,β-unsaturated ester MA, μ = –0.1586 au, thereby indicating that the net charge-transfer will take place from the silyl enol ether to the α,β-unsaturated ester, in agreement with the charge-transfer analysis (vide infra). Coordination of the LA to the carbonyl oxygen atom of methyl acrylate increases the electronic chemical potential of the MA–LA complex to –0.2008 au.

Table 1. Global properties of the species considered in this work.[a]

	HOMO	LUMO	μ	η	ω	ΔN_{max}
13	–0.2854	–0.1161	–0.2008	0.1693	3.24	1.19
8	–0.2720	–0.0452	–0.1586	0.2268	1.51	0.70
7	–0.2197	0.0436	–0.0881	0.2632	0.40	0.33

[a] HOMO and LUMO energies, electronic chemical potential, and chemical hardness are given in au, with global electrophilicity values in eV.

Methyl acrylate (**8**) has an electrophilicity value of 1.51 eV, a value that falls in the range of strong electrophiles within the ω scale.[13] Coordination of the LA ($AlCl_3$) to the carbonyl oxygen atom of MA increases the electrophilicity of the MA–LA complex notably, to 3.24 eV. This fact increases the Δω for the LA-catalyzed [2+2] cycloaddition, and an acceleration of the reaction will be expected along a more polar process. The SVE has a low electrophilicity value, ω = 0.40 eV, and we will assume that it behaves as a strong nucleophile.[13] The large $\Delta\omega$ for the LA-catalyzed [2+2] cycloaddition, 2.84 eV, indicates that this cycloaddition will take place with a large polar character. Note that the $\Delta\omega$ for the cycloaddition between SVE and MA–LA complex is larger than that for the [2+2] cycloaddition between benzyne possessing a fused four-membered ring and a ketene acetal, $\Delta\omega$ = 1.7 eV, which has recently been characterized as a polar stepwise cycloaddition.[8]

The analysis of the local electrophilicity of the α,β-unsaturated ester MA and the MA–LA complex, together with the analysis of the nucleophilic Fukui functions, f_k^-, at SVE allows us to characterize the more favorable two-center interaction along an asynchronous bond-formation process, and, in consequence, the more favorable regioisomeric reactive channel.[19] The values of these local indexes are summarized in Scheme 4. MA has a larger electrophilic activation at the C1 carbon (0.63 eV) than at the C2 and C3 carbons (0.30 eV; see Scheme 4). Therefore, the C1 carbon atom, which corresponds to the β-conjugated position of a Michael acceptor,[20] is the more favorable center for a nucleophilic attack. Coordination of the LA to the carbonyl oxygen atom decreases the selectivity between the C1 and C3 carbon atoms of the MA–LA complex, but the C1 carbon atom remains the more electrophilic site of the molecule. The ω_k at the C1 carbon atom of the MA–LA complex, 1.22 eV, is twice the value of ω_k at the C1 carbon atom of MA, 0.63 eV. For the SVE, the analysis of the Fukui functions for an electrophilic attack, f_k^-, indicates that the C5 carbon atom corresponds to the more nucleophilic site of the molecule. In consequence, along a polar cycloaddition the more favorable reactive channel will correspond to that associated with a two-center interaction between the C1 carbon atom of MA–LA and the C5 carbon atom of the SVE, with formation of the 1,2-disubstituted cyclobutanes. This analysis is in complete agreement with the regioselectivity observed experimentally.[16]

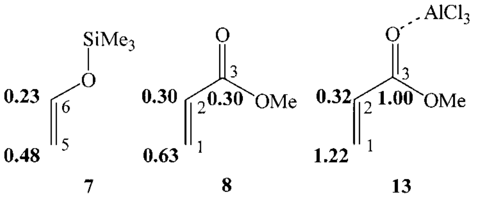

Scheme 4.

Analysis of the PES of the Cycloadditions Between Trimethylsilyl Enol Ether and Methyl Acrylate

Methyl acrylate can adopt two planar conformations – *s-trans* (**8**) and *s-cis* (**9**) – with **9** being 0.7 kcal mol^{-1} more stable than **8** (see Table 2). The reactions between the silyl enol ether **7** and MA in the two conformations have been considered. Analysis of the PES for these reactions indicates that they are concerted cycloaddition reactions that allow the formation of the corresponding [2+2] and [4+2] cycloadducts (see Scheme 5). For the reaction of the silyl enol ether **7** with MA in the *s-trans* conformation **8**, two stereoisomeric reactive channels with formation of the *cis* or *trans* 1,2-disusbtituted cyclobutanes are feasible. Thus, three TSs (**TSa**, **TSb**, and **TSc**), two [2+2] cycloadducts (**10** and **11**), and one [4+2] cycloadduct (**12**) have been located and characterized. The stationary points corresponding to the [2+2] and [4+2] cycloaddition reactions between SVE and MA in the *s-trans* **8** and the *s-cis* **9** conformations are shown in Scheme 5 together with the atom numbering. The total and relative energies are summarized in Table 2. The geometries of the TSs are given in Figure 1.

Table 2. Total [au] and relative[a] [kcal mol^{-1}] energies, E, and enthalpies, H, in vacuo, and total (E_{sol} [au]) and relative[a] (ΔE_{sol} [kcal mol^{-1}]) energies in dichloromethane for the cycloaddition reactions between enol ether **7** and MA and the MA–LA complex.

	E	ΔE	H	ΔH	E_{sol}	ΔE_{sol}
7	–562.524023		–562.365705		–562.525637	
8	–306.466612		–306.370437		–306.469382	
9	–306.467760		–306.371598		–306.470420	
13	–1929.753867		–1929.648083		–1929.763292	
14	–1929.753262		–1929.646928		–1929.761966	
TSa	–868.931896	36.9	–868.675518	38.0	–868.941283	33.7
TSb	–868.930533	37.7	–868.674407	38.7	–868.940900	34.0
TSc	–868.960366	19.7	–868.703634	21.1	–868.962184	21.3
10	–869.022629	–20.1	–868.762096	–16.3	–869.025501	–19.1
11	–869.020414	–18.7	–868.759874	–14.9	–869.023412	–17.8
12	–869.010436	–11.7	–868.749733	–7.8	–869.011856	–9.9
TS1-1	–2492.263013	9.3	–2491.995610	11.4	–2492.275031	8.7
TS1-2	–2492.261759	10.1	–2491.994582	12.1	–2492.274276	9.2
TS1-3	–2492.269799	5.1	–2492.002493	7.1	–2492.279448	5.9
TS1-4	–2492.265685	7.7	–2491.998466	9.6	–2492.276388	7.9
IN-1	–2492.265936	7.5	–2491.998688	9.5	–2492.279022	6.2
IN-2	–2492.266188	7.3	–2491.997403	10.3	–2492.281968	4.4
IN-3	–2492.273801	2.6	–2492.004691	5.7	–2492.284463	2.8
IN-4	–2492.269833	5.1	–2492.001030	8.0	–2492.282527	4.0
TS2-1	–2492.263020	9.3	–2491.995391	11.5	–2492.277627	7.1
TS2-2	–2492.262847	9.4	–2491.994919	11.8	–2492.278912	6.3
TS2-3	–2492.266004	7.5	–2491.998299	9.7	–2492.279997	5.6
TS2-4	–2492.273564	2.7	–2492.004675	5.7	–2492.282141	4.3
TS2-5	–2492.262068	9.9	–2491.994691	12.0	–2492.275461	8.5
TS2-6	–2492.269052	5.5	–2492.000310	8.5	–2492.279657	5.8
15	–2492.310279	–20.3	–2492.039592	–16.2	–2492.319091	–18.9
16	–2492.310101	–20.2	–2492.039432	–16.1	–2492.318169	–18.3
17	–2492.276594	0.8	–2492.006305	4.7	–2492.282146	4.3
18	–2492.272935	3.1	–2492.002650	7.0	–2492.279766	5.8

[a] Relative to **7** plus **8** or **9**, and to **7** plus **13** or **14**.

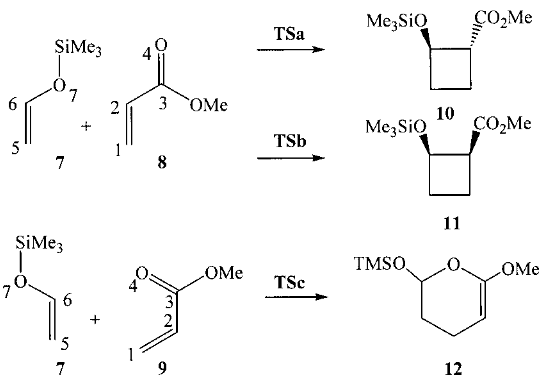

Scheme 5.

The activation enthalpies associated with the [2+2] cycloadditions between the SVE and the *s-trans* conformation of

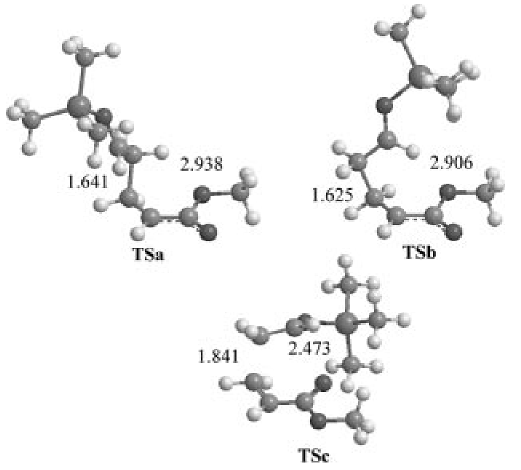

Figure 1. Transition structures involved in the [2+2] cycloadditions (**TSa** and **TSb**) and the [4+2] cycloaddition (**TSc**) between the silyl enol ether **7** and the *s-trans* and *s-cis* conformations of methyl acrylate. The interatomic distances between centers directly involved in the bond-forming processes are given in Å.

MA (**8**) are 38.0 (**TSa**) and 38.7 (**TSb**) kcal mol^{-1}, respectively. These unfavorable energies prevent the [2+2] cycloaddition between SVE and **8**. The formation of cyclobutanes **10** and **11** is an exothermic process by –16.3 and –14.9 kcal mol^{-1}, respectively. The *trans*-1,2-disubstituted cyclobutane **10** is therefore 1.4 kcal mol^{-1} more stable than the *cis* one (**11**). The activation enthalpy associated with the [4+2] cycloaddition between the *s-cis* conformation of MA (**9**) and the SVE via **TSc** is 21.1 kcal mol^{-1}. This activation energy is lower than that computed for the acrolein + ethylene [4+2] cycloaddition reaction (ΔE = 24.0 kcal mol^{-1})[21] as a consequence of the larger nucleophile character of SVE than ethylene. The [4+2] cycloaddition is exothermic by –7.8 kcal mol^{-1}.

The geometries of the TSs are presented in Figure 1. The lengths of the C1–C5 and C2–C6 forming bonds at the TSs associated with the [2+2] cycloadditions are 1.641 and 2.938 Å (**TSa**), and 1.625 and 2.906 Å (**TSb**). The lengths of the C1–C5 and O4–C6 forming bonds at the TS associated with the [4+2] cycloaddition, **TSc**, are 1.841 and 2.473 Å, respectively. The extent of the asynchronicity of the bond formation can be measured by means of the difference between the lengths of the two σ bonds that are being formed in the reaction, i.e $\Delta r = d(\text{C1–C5}) - d(\text{C2–C6})$. These values, Δr = 1.30 for **TSa**, Δr = 1.28 for **TSb**, and Δr = 0.62 for **TSc**, indicate that these TSs correspond to highly asynchronous bond-formation processes, where the C1–C5 forming bond at the β-position of MA is being formed to a large extent as a consequence of the large polarization of the C1–C2 double bond of MA. The TSs associated with the [2+2] cycloaddition processes are more asynchronous than that associated with the [4+2] one.

The natural population analysis (NPA) allows us to evaluate the charge transfer (CT) along the nucleophilic attack of the SVE to MA. The natural charges at the TSs appear to be shared between the donor SVE and the acceptor MA. The CT from SVE to MA at the TSs are: 0.42 e at **TSa**, 0.40 e at **TSb**, and 0.33 e at **TSc**. These values, which indicate that these species have some zwitterionic character, are in agreement with the large dipole moment of the TSs associated with the [2+2] cycloadditions, namely 7.66 D (**TSa**) and 8.47 D (**TSb**). The TS associated with the [4+2] cycloaddition, **TSc**, presents a lower CT and a lower dipole moment (3.17 D) as a consequence of the back-donation along the O4–C6 bond formation.

As these cycloadditions have a large polar character, and solvent effects can have some incidence on the energies, the solvent effects have been considered by B3LYP/6-31G* single-point calculations on the gas-phase stationary points using a relatively simple polarizable continuum model. The total and relative energies are summarized in Table 2. Solvent effects stabilize all stationary points between 1.0 and 6.5 kcal mol^{-1}. The TSs associated with the [2+2] processes are stabilized more than the reagents due to the large zwitterionic character of the former. In consequence, the inclusion of the solvent effects decreases the gas-phase barriers for the [2+2] cycloadditions by around 4 kcal mol^{-1}. A different behavior is found for the [4+2] cycloaddition, where the activation barrier increases by 1.5 kcal mol^{-1} as a consequence of a larger stabilization of the reagents than **TSc**.

Analysis of the PES of the Cycloadditions Between Trimethylsilyl Enol Ether and the Methyl Acrylate–AlCl$_3$ Complex

Analysis of the results indicate that the LA-catalyzed [2+2] cycloaddition between SVE and the MA–LA complex takes place along a stepwise process, the first step being the nucleophilic attack of SVE to the MA–LA complex. For this step, which corresponds to a two-center addition, several approach modes are feasible, related to the attack of SVE to the *s-cis* and the *s-trans* conformation of MA and the formation of the *cis*- and *trans*-1,2-disubstituted cyclobutanes. All four possibilities have been considered. In addition, for the channels associated with the attack of SVE to the MA–LA complex in the *s-cis* conformation, two reactive channels associated with the formation of the six-membered heterocarbocycle have also been considered.[22] Thus, four TSs associated with the nucleophilic attack of SVE to the MA–LA complex (**TS1-1**, **TS1-2**, **TS1-3**, and **TS1-4**), four zwitterionic intermediates (**IN-1**, **IN-2**, **IN-3**, and **IN-4**), and six TSs corresponding to the cyclization step (**TS2-1**, **TS2-2**, **TS2-3**, **TS2-4**, **TS2-5,** and **TS2-6**) and their corresponding cycloadducts, have been located and characterized on the PES. The stationary points corresponding to the cycloaddition between SVE and the MA–LA complex are shown in Scheme 6 together with the atom numbering, total and relative energies are summarized in Table 2, and the geometries of the TSs are given in Figures 2 and 3.

The activation enthalpies associated with the nucleophilic attack of SVE at the C1 carbon of the MA–LA complex in the *s-cis* and *s-trans* conformations are between 7.1 and 12.1 kcal mol^{-1}. The attack on MA–LA complex in the

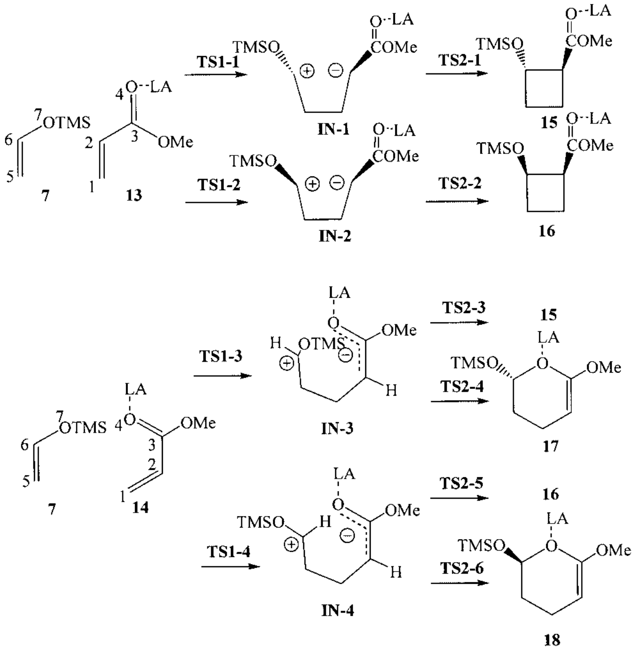

Scheme 6.

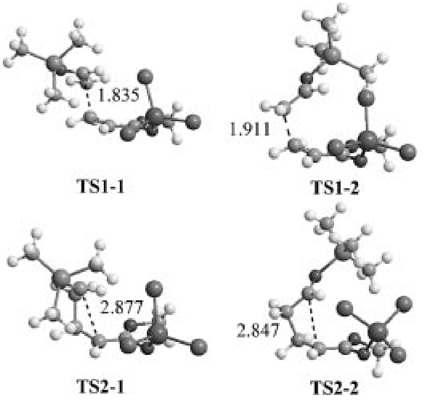

Figure 2. Transition structures involved in the LA-catalyzed cycloaddition between the silyl enol ether **7** and the MA–LA complex in the *s-trans* conformation (**13**). The interatomic distances between centers directly involved in the bond-forming processes are given in Å.

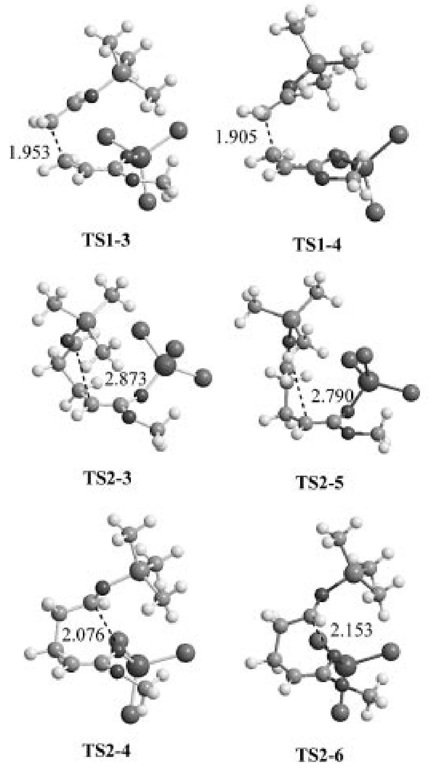

Figure 3. Transition structures involved in the LA-catalyzed cycloaddition between the silyl enol ether **7** and the MA–LA complex in the *s-cis* conformation (**14**). The interatomic distances between centers directly involved in the bond forming processes are given in Å.

s-cis conformation is 2–5 kcal mol^{-1} more favorable than the attack on the *s-trans* one. The activation enthalpy associated with **TS1-3** (7.1 kcal mol^{-1}) is 14.0 kcal mol^{-1} lower in energy than that associated with **TSc**. Therefore, coordination of the LA to the carbonyl oxygen atom of MA produces a drastic acceleration of the reaction. This result is in complete agreement with the increase of $\Delta\omega$ for the catalytic reaction (see above), and with the fact that the reaction takes place at a very low temperature (–78 °C).[16] The zwitterionic intermediate **IN-3** is located about 1.4 kcal mol^{-1} below **TS1-3**.

The second step of these cycloadditions is the ring-closure of the corresponding zwitterionic intermediates. This process takes place with formation of the second σ-bond between the more electrophilic and nucleophilic centers of these zwitterionic intermediates. Since the negative charge of these zwitterionic intermediates is mainly localized at the C2 carbon atom and the O4 oxygen atom of the MA residue, the subsequent bond-formation can take place by two alternative channels corresponding to the ring closure between the C6 carbon atom of the vinyl ether and the C2 carbon atom or the carbonyl O4 oxygen atoms of MA, with formation of the formal [2+2] and [4+2] cycloadducts, respectively. Note that along the channels associated with the attack of MA on the *s-trans* conformation the formation of the six-membered cycloadducts is geometrically not feasible.

Analysis of the energetic results given in Table 2 shows that the intermediate **IN-3**, which has an inappreciable barrier, yields the [4+2] cycloadduct **17** via **TS2-4**. However, formation of **17** is endothermic by 4.7 kcal mol^{-1}. In consequence, although the [4+2] cycloadduct **17** is the product of kinetic control, it reverts to reagents with a very low barrier of 1.0 kcal mol^{-1}. Note that the [4+2] cycloadduct is not observed experimentally. On the other hand, the intermediate **IN-3**, with a barrier of 4.0 kcal mol^{-1}, yields the [2+2] cycloadduct **15** via **TS2-3**. In this case, the exothermic character of the process (–16.2 kcal mol^{-1}) makes the reaction essentially irreversible. The relative enthalpies of the TSs associated with the formation of the *trans*-1,2-disubstituted cyclobutane **15** via **TS1-3** and **TS2-3** are 2.5 and

2.3 kcal mol^{-1} lower in energy than those associated with the formation of the *cis*-1,2-cyclobutane **16** via **TS1-4** and **TS2-5**, respectively. These energetic results are in reasonable agreement with the greater formation of the *trans* isomers than the *cis* ones.[16]

The geometries of the TSs are presented in Figures 2 and 3. The lengths of the C1–C5 forming bonds at the TSs associated with the nucleophilic attack of SVE on the MA–LA complex are 1.835 Å (**TS1-1**), 1.911 Å (**TS1-2**), 1.953 Å (**TS1-3**), and 1.905 Å (**TS1-4**), while the distance between the C2 and C6 or O4 atoms are larger than 3 Å. These geometrical parameters indicate that these TSs correspond to a two-center addition associated with a Michael-type addition of the vinyl ether to the β-conjugated position of the MA–LA complex. At the zwitterionic intermediates, the lengths of the C1–C5 bonds are 1.56 and 1.60 Å, while the distances between the C2 and C6 or O4 atoms remain larger than 2.8 Å. Finally, at the TSs associated with the ring-closure process with formation of the [2+2] cycloadducts the lengths of the C2–C6 forming bonds are 2.877 Å (**TS2-1**), 2.847 Å (**TS2-2**), 2.873 Å (**TS2-3**), and 2.790 Å (**TS2-5**), while at the TSs associated with the formation of the [4+2] cycloadducts the length of the O4–C6 forming bond are 2.076 Å (**TS2-4**) and 2.153 Å (**TS2-6**).

The NPA allows us to evaluate the CT along the nucleophilic attack of the SVE on the MA–LA complex. The natural charges at the TSs are shared between the donor SVE and the acceptor MA–LA complex. The charge transferred from the SVE to the MA–LA complex is 0.52 e at **TS1-1**, 0.46 e at **TS1-2**, 0.43 e at **TS1-3**, 0.46 e at **TS1-4**, 0.75 e at **IN-1**, 0.74 e at **IN-2**, 0.75 e at **IN-3**, and 0.74 e at **IN-4**. These values indicate that these species have a large zwitterionic character. The CT increases along the nucleophilic attack of SVE on the MA–LA complex, with a maximum value at the corresponding intermediates. These values are in agreement with the large dipole moment of these intermediates of between 12 and 15 D. The increase of the charge transfer in the LA-catalyzed process is in agreement with the larger electrophilicity value of the MA–LA complex than MA (see above).

Solvent effects stabilize all stationary points between 3.5 and 10.1 kcal mol^{-1}. The TSs and intermediates are stabilized more than the reagents due to the large zwitterionic character of the former. However, the solvent effect has a lesser effect in the activation energy due to the large solvation of the MA–LA complex (5.9 kcal mol^{-1}). In consequence, the inclusion of solvent effects decreases the gas-phase barrier by around 1 kcal mol^{-1}. In dichloromethane, formation of the [4+2] cycloadduct **17** remains 4.3 kcal mol^{-1} above the reactants, while the [2+2] cycloadduct **15** is 18.9 kcal mol^{-1} below the reactants.

Conclusions

The LA-induced [2+2] cycloaddition of trimethysilyl vinyl ether with methyl acrylate has been studied by DFT methods at the B3LYP/6-31G* level. In the absence of an LA, a [4+2] cycloaddition between the silyl enol ether and methyl acrylate in the *s-cis* conformation takes place through an asynchronous, concerted bond-formation process. This cycloaddition has a large activation enthalpy of 21.1 kcal mol^{-1}.

Coordination of the LA to the carbonyl oxygen atom of MA changes the mechanism and produces a drastic acceleration of the reaction. The LA-catalyzed cycloaddition takes place along a polar, stepwise mechanism initiated by the nucleophilic attack of the SVE at the conjugated β-position of MA. This large acceleration can be related to the increase of the electrophilicity of the LA-coordinated α,β-unsaturated ester, which favors the cycloaddition by a polar process. The ring-closure of the zwitterionic intermediates associated with the addition of the enol ether to the MA–LA complex in the *s-cis* conformation takes place with an inappreciable activation energy to give the [4+2] cycloadducts. However, while the formation of the [4+2] cycloadducts is kinetically favored, formation of the [2+2] cycloadducts is thermodynamically very favored. The ratio of formation of the *cis*- and *trans*-cyclobutanes found for the catalyzed process is in reasonable agreement with the experimental outcome.

The present study shows that these polar cycloadditions are promoted by a nucleophile/electrophile interaction between the electron-rich π-system of the silyl enol ether and the electron-deficient π-system of the methyl acrylate–Lewis acid complex, while formation of the formal [*m*,*n*] cycloadducts is decided at the ring-closure step. Both kinetic or thermodynamic controls can be responsible for the *pseudo-periselectivity* observed experimentally.

Computational Methods

DFT calculations were carried out using the B3LYP[23] exchange-correlation functionals, together with the standard 6-31G* basis set.[24] The optimizations were carried out using the Berny analytical gradient optimization method.[25] The stationary points were characterized by frequency calculations in order to verify that the transition structures had only one imaginary frequency. The intrinsic reaction coordinate (IRC)[26] path was traced in order to check the energy profiles connecting each transition structure to the two associated minima of the proposed mechanism by using the second-order González–Schlegel integration method.[27] The electronic structures of stationary points were analyzed by the natural bond orbital (NBO) method.[28] All calculations were carried out with the Gaussian 98 suite of programs.[29] The values of the relative enthalpies were calculated based on the total energies and the thermochemical analysis at the B3LYP/6-31G* level. The thermal contributions to the vibrational energy were scaled by 0.96.[30] The energies were computed at –78 °C, and the enthalpies were calculated with the standard statistical thermodynamic formulae.[24] The solvent effects, modeled as a continuum model, were considered by B3LYP/6-31G* single-point calculations on the gas-phase optimized geometries using a relatively simple self-consistent reaction field (SCRF)[31] based on the polarizable continuum model (PCM) of Tomasi's group.[32] Since these cycloadditions are carried out in dichloromethane, we selected its dielectric constant at 298.0 K (ε = 8.93).

Acknowledgments

This work was supported by research funds provided by the Ministerio de Ciencia y Tecnología of the Spanish Government by DGICYT (project BQU2002-01032) and by the AVCYT of the Generalitat Valenciana (reference GRUPOS03/176).

---

[1] a) R. Huisgen, R. Grashey, J. Sauer, *The Chemistry of Alkenes*, Wiley, London, **1964**; b) W. Carruthers, *Cycloaddition Reactions in Organic Synthesis* Pergamon, Oxford, **1990**; c) A. Padwa, *Comprehensive Organic Chemistry*, Pergamon, Oxford, **1991**, p. 1069–1109; d) A. Padwa, *1,3-Dipolar Cycloaddition Chemistry*, Wiley-Interscience, New York, **1984**; e) S. Kobayashi, K. A. Jorgensen, *Cycloaddition Reactions in Organic Synthesis*, Wiley-VCH, Weinheim, **2002**.

[2] a) I. Fleming, *Frontier Orbitals, Organic Chemical Reactions*, John Wiley and Sons, New York, **1976**; b) K. N. Houk, J. González, Y. Li, *Acc. Chem. Res.* **1995**, *28*, 81.

[3] a) R. B. Woodward, R. Hoffmann, *Angew. Chem. Int. Ed. Engl.* **1969**, *8*, 781; b) R. B. Woodward, R. Hoffmann, *The Conservation of Orbital Symmetry*, Verlag Chemie, Weinheim, **1970**.

[4] O. Diels, K. Alder, *Justus Liebigs Ann. Chem.* **1928**, *460*, 98.

[5] a) R. Sustmann, W. Sicking, *J. Am. Chem. Soc.* **1996**, *118*, 12562; b) R. Sustmann, S. Tappanchai, H. Bandmann, *J. Am. Chem. Soc.* **1996**, *118*, 12555; c) L. R. Domingo, M. T. Picher, R. J. Zaragozá, *J. Org. Chem.* **1998**, *63*, 9183.

[6] J. A. Sáez, M. Arnó, L. R. Domingo, *Org. Lett.* **2003**, *5*, 4117.

[7] L. R. Domingo, M. T. Picher, *Tetrahedron* **2004**, *60*, 5053.

[8] L. R. Domingo, P. Pérez, R. Contreras, *Lett. Org. Chem.* **2005**, *2*, 68.

[9] a) R. Lopez, D. Suarez, T. L. Sordo, M. F. Ruiz-Lopez, *Chem. Eur. J.* **1998**, *4*, 328; b) B. Lecea, A. Arrieta, I. Arrastia, F. P. Cossio, *J. Org. Chem.* **1998**, *63*, 5216; c) A. Arrieta, B. Lecea, F. P. Cossio, *J. Org. Chem.* **1998**, *63*, 5869; d) M. Alajarin, A. Vidal, F. Tovar, A. Arrieta, B. Lecea, F. P. Cossio, *Chem. Eur. J.* **1999**, *5*, 1106; e) D. V. Deubel, S. Schlecht, G. Frenking, *J. Am. Chem. Soc.* **2001**, *123*, 10085; f) C. Zhou, D. M. Birney, *J. Am. Chem. Soc.* **2002**, *124*, 5231; g) D. A. Singleton, Y. C. Wang, H. W. Yang, D. Romo, *Angew. Chem. Int. Ed.* **2002**, *41*, 1572; h) P. Brana, J. Gimeno, J. A. Sordo, *J. Org. Chem.* **2004**, *69*, 2544.

[10] H.-O. Ho, W. K. Li, *J. Mol. Struct. (Theochem)* **2004**, *712*, 49.

[11] a) S. M. Bachrach, J. C. Gilbert, D. W. Laird, *J. Am. Chem. Soc.* **2001**, *123*, 6706; b) S. M. Bachrach, J. C. Gilbert, *J. Org. Chem.* **2004**, *69*, 6357; c) I. Ozkan, A. Kinal, *J. Org. Chem.* **2004**, *69*, 5390.

[12] R. G. Parr, L. von Szentpaly, S. Liu, *J. Am. Chem. Soc.* **1999**, *121*, 1922.

[13] L. R. Domingo, M. J. Aurell, P. Pérez, R. Contreras, *Tetrahedron* **2002**, *58*, 4417.

[14] P. Pérez, L. R. Domingo, M. J. Aurell, R. Contreras, *Tetrahedron* **2003**, *59*, 3117.

[15] a) R. Huisgen, H. Rist, *Justus Liebigs Ann. Chem.* **1955**, *594*, 137; b) R. A. Benkeser, C. E. DeBoer, *J. Org. Chem.* **1956**, *21*, 281.

[16] K. Takasu, M. Ueno, K. Inanaga, M. Ihara, *J. Org. Chem.* **2004**, *69*, 517.

[17] J. A. Ross, R. P. Seiders, D. M. Lemal, *J. Am. Chem. Soc.* **1976**, *98*, 4325.

[18] a) R. G. Parr, R. G. Pearson, *J. Am. Chem. Soc.* **1983**, *105*, 7512; b) R. G. Parr, W. Yang, *Density Functional Theory of Atoms and Molecules*, Oxford University Press, New York, **1989**.

[19] L. R. Domingo, M. J. Aurell, P. Pérez, R. Contreras, *J. Phys. Chem. A* **2002**, *106*, 6871.

[20] L. R. Domingo, P. Pérez, R. Contreras, *Tetrahedron* **2004**, *60*, 6585.

[21] Y. S. Park, B.-S. Lee, I. Lee, *New J. Chem.* **1999**, *23*, 707.

[22] S. Yamabe, T. Minato, *J. Org. Chem.* **2000**, *65*, 1830.

[23] a) A. D. Becke, *J. Chem. Phys.* **1993**, *98*, 5648; b) C. Lee, W. Yang, R. G. Parr, *Phys. Rev. B* **1988**, *37*, 785.

[24] W. J. Hehre, L. Radom, P. v. R. Schleyer, J. A. Pople, *Ab initio Molecular Orbital Theory*, Wiley, New York, **1986**.

[25] a) H. B. Schlegel, *J. Comput. Chem.* **1982**, *3*, 214; b) H. B. Schlegel, "Geometry Optimization on the Potential Energy Surface" in *Modern Electronic Structure Theory* (Ed.: D. R. Yarkony), World Scientific Publishing, Singapore, **1994**.

[26] K. Fukui, *J. Phys. Chem.* **1970**, *74*, 4161.

[27] a) C. González, H. B. Schlegel, *J. Phys. Chem.* **1990**, *94*, 5523; b) C. González, H. B. Schlegel, *J. Chem. Phys.* **1991**, *95*, 5853.

[28] a) A. E. Reed, R. B. Weinstock, F. Weinhold, *J. Chem. Phys.* **1985**, *83*, 735; b) A. E. Reed, L. A. Curtiss, F. Weinhold, *Chem. Rev.* **1988**, *88*, 899.

[29] M. J. Frisch, G. W. Trucks, H. B. Schlegel, G. E. Scuseria, M. A. Robb, J. R. Cheeseman, V. G. Zakrzewski, J. Montgomery, J. A., R. E. Stratmann, J. C. Burant, S. Dapprich, J. M. Millam, A. D. Daniels, K. N. Kudin, M. C. Strain, O. Farkas, J. Tomasi, V. Barone, M. Cossi, R. Cammi, B. Mennucci, C. Pomelli, C. Adamo, S. Clifford, J. Ochterski, G. A. Petersson, P. Y. Ayala, Q. Cui, K. Morokuma, D. K. Malick, A. D. Rabuck, K. Raghavachari, J. B. Foresman, J. Cioslowski, J. V. Ortiz, B. B. Stefanov, G. Liu, A. Liashenko, P. Piskorz, I. Komaromi, R. Gomperts, R. L. Martin, D. J. Fox, T. Keith, M. A. Al-Laham, C. Y. Peng, A. Nanayakkara, M. Challacombe, P. M. W. Gill, B. Johnson, W. Chen, M. W. Wong, J. L. Andres, C. Gonzalez, M. Head-Gordon, E. S. Replogle, J. A. Pople *Gaussian 98*, Revision A.6, Gaussian, Inc., Pittsburgh PA, **1998**.

[30] A. P. Scott, L. Radom, *J. Phys. Chem.* **1996**, *100*, 16502–16513.

[31] a) J. Tomasi, M. Persico, *Chem. Rev.* **1994**, *94*, 2027; b) B. Y. Simkin, I. Sheikhet, *Quantum Chemical and Statistical Theory of Solutions − A Computational Approach*, Ellis Horwood, London, **1995**.

[32] a) E. Cances, B. Mennucci, J. Tomasi, *J. Chem. Phys.* **1997**, *107*, 3032; b) M. Cossi, V. Barone, R. Cammi, J. Tomasi, *Chem. Phys. Lett.* **1996**, *255*, 327; c) V. Barone, M. Cossi, J. Tomasi, *J. Comput. Chem.* **1998**, *19*, 404.

Received: March 11, 2005